Highly selective and robust nanocomposite-based sensors for potassium ions detection

Antonio Ruiz-Gonzalez, Kwang Leong Choy*

ABSTRACT

Ion-selective electrodes are employed in technological important fields, such as medical diagnosis, or water quality evaluation. Plasticized polymeric membranes containing ionophores are typically used in these devices. However, the low mechanical hardness and limited robustness of these electrodes combined with their low selectivity limit their use in high precision applications. In the present work, PVC-functionalised silica nanoparticles incorporated in a plasticized PVC film have been integrated into ion sensors for the first time applied to the detection of K^+ in solution. This approach was used for the design of highly specific and mechanically robust systems using a fluidic chamber. The device presented a hardness in the range of 5.2 GPa, being 2 orders of magnitude higher than the one reported for plasticized PVC (0.059 GPa), and could measure the concentration of K^+ with high specificity when compared to Ca^{2+} and Na^+ ions compared to the conventional approach. The interactions of the sensing films with the ions in solution were systematically studied for different degrees of PVC functionalisation to allow the rational design of a robust and selective sensor. The final device exhibited one of the lowest signal drift ever reported, with 1.3 $\mu V\ h^{-1}$. The system operated under fluid pressure and shear stress conditions of 45 mbar for at least 8 h while the control experiment, fabricated using the conventional composition without nanoparticles showed a significantly higher noise (circa 115.6 $\mu V\ h^{-1}$) and degraded after 4 h of continuous measurements. The sensors here reported could also be used for the accurate determination of the concentration of K^+ inside complex mixtures of ions such as simulated body fluids and human serum, leading to a plethora of applications in healthcare for the diagnosis and monitoring of diseases.

Keywords: Polymer functionalisation, Nanocomposite, Ion-selective electrode, additive manufacturing, background noise

1. INTRODUCTION

Ion-selective electrodes (ISEs) are currently employed in multiple fields including [1], medical diagnosis [2], or water quality assessment [3]. In addition, potassium ions are essential in the cell homeostasis, neuronal function [4] and audition [5] among others. Thus, its measurement represents a powerful diagnostic tool for the detection of multiple conditions such as dehydration [6] and cardiovascular diseases [7], which are some of the most common affections within the grown population [8].

Despite the severity of this condition, there is not a universally accepted definition for dehydration, and no clinical methods are currently employed for its evaluation. In fact, the number of people affected by electrolyte unbalances is expected to increase due to high dietary potassium [9], and the increasing use of certain drugs, including Acetylcholinesterase (ACE) inhibitors [10], which affects the hormones responsible for the excretion of diluted ions by the kidneys. Thus, a system for the continuous measurement of electrolytes, especially potassium ions, is highly desirable.

The determination of the concentration of ions in solution can be accomplished by the use of materials and nanomaterials that can selectively bind ions such as bismuth terephthalate metal-organic frameworks, for the detection of Pb^{2+} and Cd^{2+} [11] or iridium oxide, which can be used for the measurement of pH [12]. To date, a plasticized PVC film where one or more ionophores are embedded represents the preferred option for the fabrication of ion sensors [13]. These sensors have been adapted to wearable technologies, allowing the real-time monitoring of physiological markers [14], and implanted devices [15]. However, the signal noise of these approaches is high due to the susceptibility to mechanical stress and the presence of interference electrolytes present in most biological samples [14]. Although PVC has a good biocompatibility, being employed in multiple medical devices such as catheters and peritoneal dialysis bags [16], it can degrade over

time, releasing Cl^- and oxygen radicals [17]. The integration of biopolymers such as gelatin hydrogels with incorporated silver nanoparticles, and Poly(acrylonitrile-co-acrylic acid) Composites have been proven to enhance the biological applications of nanocomposites by improving their antibacterial properties [18, 19], these materials have not been applied to ion sensing yet. However, multiple alternatives to PVC have been adapted within recent years such as polyacrylate [20], polyurethane [21] and organosilicon compounds [22], showing a Nernstian sensitivity. However, due to the limited ionic diffusion inside these polymeric membranes, the equilibration times are high, up to months or years, than the conventional PVC-based membranes, which normally reaches an equilibrium after 12 h [23].

Typical ion sensors employ a plasticizer such as bis-(2-ethylhexyl) sebacate or o-nitrophenyl octyl ether that not only increases the ionic conductivity [24], but also improves the elasticity of the films, and avoids the spontaneous formation of cracks in PVC. However, the use of plasticizers also reduces the hardness and robustness of the films, which becomes an impediment when employing the sensors for specific applications such as in wearable technologies due to the friction with the skin [25] or their use in implanted devices because of the high shear stress of the circulating blood [26]. Nevertheless, there is limited literature on the improvement of hardness and mechanical resilience of ion sensors. To date, only some early work in the field have been performed, modifying the composition of the films by incorporating plasticizers such as didecylphosphoric acid to increase the hardness [27, 28].

The performance of ISEs is determined by the ionic exchange capabilities of the polymeric films. Therefore, both sensitivity and ionic interferences effects are highly dependent on the composition of the films, especially regarding the selected plasticizer, the polymer, as well as the ionophore.

The current advances in nanotechnology have allowed a rapid expansion of the field of ion sensors by enhancing the surface properties of the polymer films through the formation of nanocomposites. Such nanocomposites have allowed the fabrication of anti-flammable [29] and high-performance

dielectric materials [30] among others. Such nanomaterials could reduce the charge transfer resistance of the sensing films, improving the performance of the sensors. In the field of ion-selective electrodes, a few examples using metal oxide-based nanoparticles can be found, such as TiO_2 in a plasticized PVC matrix for the measurement of Cr^{3+} [31] and platinum nanoparticles in a polyacrylate film for the detection of K^+, with improved stability due to the lower electrical resistivity of the films [32]. This device incorporating platinum nanoparticles exhibited a standard deviation of the potentiometric signal in the range of 2 mV. In addition, the implementation of gold nanoclusters inside the plasticizer PVC films reduced the noise levels of the sensors to 10.2 $\mu V\ h^{-1}$ for the detection K^+, one of the lowest reported values for signal stability in the literature [33].

The incorporation of silica nanoparticles could represent a step further in the field, since they are chemically stable and biocompatible, and they can be easily functionalised with multiple chemical groups to tailor their surface properties [34]. Silica nanoparticles can be functionalised to enhance its surface properties by increasing the hydrophobicity and preventing the diffusion of corrosive substances [35]. In addition, functionalised silica nanoparticles with polybenzimidazole groups have been incorporated in pure polybenzimidazole polymers to form nanocomposites to improve the tensile strength and adsorption capabilities of 40-60 μm thick ion-exchange membranes for the extraction of protons in aqueous media [36]. Such functionalisation could potentially not only increase the selectivity, but also the mechanical properties of the sensing films. Furthermore, the use of functionalised nanoparticles has been demonstrated to lead to a better pore interconnectivity in polymer and increase the number of ionic sites. This has been demonstrated by Tong *et al.* [37], employing sulfate-functionalised silica nanoparticles incorporated in sulfonated poly(phenylene oxide) for the adsorption of protons in water.

In particular, the field of polymer-functionalised silica nanoparticles incorporated into mechanically resilient nanocomposite films for ion exchange and water decontamination is raising

a great interest in the recent years due to their improved mechanical properties and biocompatibility [38]. The mechanical properties of the silica nanoparticles are a consequence of the improved interaction strength of the functionalised silica nanoparticulate fillers with the polymeric matrix in the nanocomposite. As a consequence, their dispersion in nanocomposites and mechanical robustness increases [39]. Silica nanoparticles covalently grafted to the matrix of poly(ethylene oxide) by using 3-glycidoxypropyltrimethoxysilane as a linker have been demonstrated to improve the ionic conductivity and the electrochemical performance of solid polymer electrolytes when using a poly-ethylene oxide matrix [40]. As such, it represents a promising approach for the design of highly friction resistant ion-selective electrodes due to the possibility of obtaining a better surface compatibility between the nanoparticles and the polymeric film. However, to the best of our knowledge, no studies have been reported on the effects of the nanocomposite consisting of functionalised silica incorporated into PVC-based inside ion-selective electrodes to improve the selectivity and mechanical robustness of the devices.

Within the present work, the impact of the incorporation -functionalised silica nanoparticles in plasticized PVC films on the mechanical stability and structural properties of the films as well as the sensing performance was determined for the first time. Different amount of PVC covalently attached on the surface of the silica nanoparticles were tested by reducing the concentration of the EDC/NHS cross-linker. These silica nanoparticles functionalised with PVC were incorporated into a plasticized PVC-based sensing film. The improvement in the mechanical hardness and elasticity as well as the sensing performance of the films in terms of sensitivity, selectivity and background noise were determined. In addition, the interactions between the nanocomposite sensing films and the electrolytes in solution were characterised. This study of the impact of different degree of grafting of PVC onto the silica nanoparticles in the sensing performance was also used to unveil the influence of the interface interactions between nanoparticles and polymers on the ion sensors, thus allowing the rational design of mechanically robust nanocomposites that could be used as

potassium ion-selective electrodes. Such robust nanocomposites could be incorporated into low-cost fluidic chambers fabricated by additive manufacturing techniques which could be used to test the resilience of the sensors. The selectivity of the sensors was finally tested by using simulated body fluids and human plasma, as a proof-of-concept for their integration in diagnostic devices.

2. MATERIALS AND METHODS

2.1 Materials

All the reagents were purchased from Sigma Aldrich unless specified; 7 nm fused silica nanoparticles, carboxylated PVC (1.8 % carboxyl basis), high molecular weight PVC (Mw ~80000), bis (2-ethyl-hexyl) sebacate (≥97.0% purity), 1-ethyl-3-(3 dimethyl aminopropyl) carbodiimide hydrochloride (EDC, commercial grade), N-hydroxysuccinimide (NHS, ~98% purity), silica glass slides, cyclohexanone (99% purity), dimethyl formamide (DMF, ≥99% purity), human serum (from human male AB plasma). Polydimethylsiloxane (PDMS, standard purity grade) was purchased from Dow Corning and Valinomycin was from MP Biomedicals (≥93% purity). Simulated body fluids were purchased from Xi'an Hat Biotechnology Co.

2.2 Functionalisation of silica nanoparticles

Commercial as-received 7 nm silica nanoparticles were first functionalised with amine groups by dispersing these nanoparticles (100 mg) into a solution of methanol (10 mL) containing aminopropyl triethoxysilane (APTES, 30 mM). This solution was stirred overnight, and the nanoparticles were washed twice with DMF by centrifuging the dispersion at 4000 rpm for 20 mins.

A standard EDC/NHS chemistry was employed to graft the polymeric chains of carboxylated PVC onto the functionalised silica surface. In this case, 1.8% carboxylated PVC (100 mg) was diluted in DMF (10 mL) containing the APTES-functionalised silica nanoparticles, and 0, 16, 32, 49, 65, and 81 mM of both crosslinkers (EDC and NHS) were mixed into the solution under constant

stirring to induce the grafting. These concentrations were calculated based on the total amount of carboxyl groups present on the PVC, and were labelled as 0, 20, 40, 60, 80, and 100%. Here, 100% of grafting corresponds to a concentration of cross-linker equal to the number of carboxylic groups in solution, and in the case of 0%, no EDC/NHS cross-linker was employed.

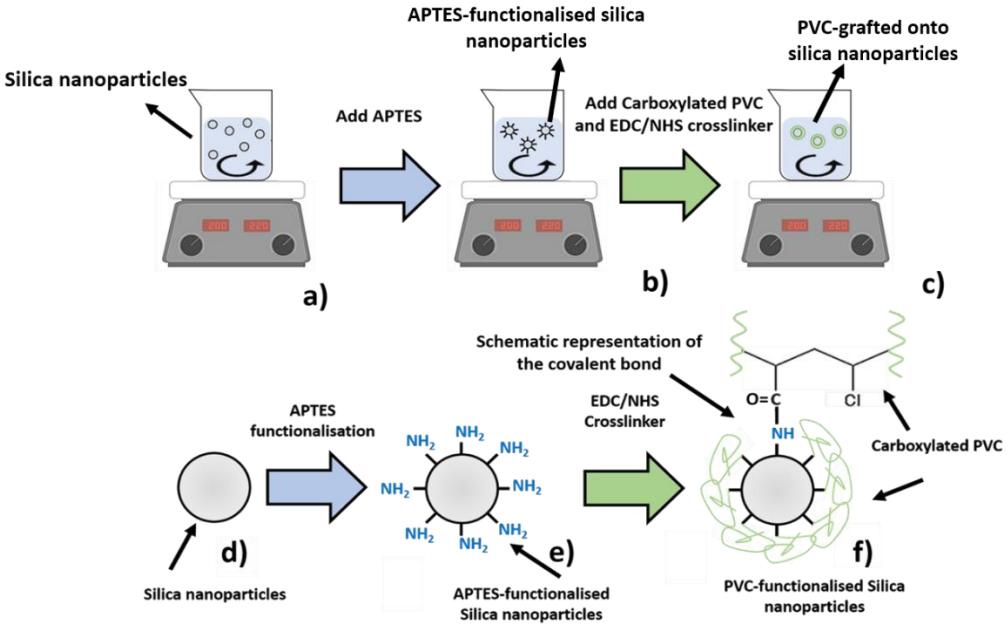

Figure 1. Schematic representations of a), b) and c) of the functionalisation process of PVC grafted onto silica nanoparticles, and the associated explanation with relevant chemical formulae in d), e) and f) **a)** Pristine silica nanoparticles are dispersed in methanol. **b)** APTES is then added into the dispersion in a) to functionalise the silica nanoparticles. APTES contains amine groups that would allow the subsequent attachment of carboxylated PVC. **c)** Carboxylated PVC is grafted on the surface of the amine functionalised silica nanoparticles by the use of EDC/NHS cross-linkers. **d)** The pristine silica nanoparticles need to be pre-treated with APTES to work as a linker for the grafting of carboxyl PVC. **e)** After functionalisation of the silica nanoparticles with APTES, amine groups are present on the surface of the nanoparticles, allowing the grafting of carboxyl PVC. **f)** Schematic representation of the final PVC polymer-grafted silica nanoparticles using the APTES as a linker for the covalent attachment of carboxylated PVC.

2.3 Characterisation of nanoparticles

The presence of polymeric chains of PVC onto the functionalised silica nanoparticles was determined by FTIR (L160000A Perkin Elmer, US). The characteristic peaks of silica and PVC were observed and compared with the patterns found in the reagents. In addition, the theoretical surface energy of the nanoparticles was established by functionalising silica glass slides with PVC using the same procedure as the nanoparticles. The contact angle of these flat surfaces was then measured using an optical tensiometer (Attension, Biolin Scientific, Sweden). The mean particle size of the PVC-functionalised silica in the cyclohexanone precursor solution was measured by using DLS (Zetasizer, Malvern Panalytical, UK) by dispersing 2 mg of nanoparticles in 1 mL of solution and measuring the particle size by triplicates.

2.4 Sensing device fabrication

For the fabrication of the sensing devices, gold electrodes with 50 nm thick were first deposited onto silica glass by sputtering (Q150R ES, Quorum technologies, UK). A polymeric film containing a solution with high molecular weight PVC (33 mg) and bis (2-ethylhexyl) sebacate (DOS, 66 mg), valinomycin (2mg) and tetraphenylborate (2mg) were then deposited by Aerosol Assisted Chemical Deposition (AACD) using a pneumatic nebuliser, adapted from the Aerosol Assisted Chemical Vapour Deposition technique [41]. This technique was used as an alternative to the conventional drop cast technique due to its versatility, low-cost, and potential mass production of the sensors with well-controlled film uniformity, structure, composition and thickness.

For the deposition of sensing films, the carboxylated PVC grafted onto functionalised silica nanoparticles were incorporated into PVC (5 wt%) and DOS (diluted in cyclohexanone) and deposited by AACD to form nanocomposite films (circa. 10 µm thick) onto gold coated glass substrates. AACD allowed the fabrication of uniform and smooth films with well controlled

surface dimensions and a low roughness. The deposition was carried out at a substrate temperature of 40 ^{o}C.

2.5 Nanocomposite characterisation

The thickness of the nanocomposite film was measured by stylus profilometer (Dektekxt, Bruker, UK), AFM (Cypher S, Oxford Instruments, UK) and SEM (EVO LS15, ZEISS, Germany) were used to characterise surface morphology of the films. The porosity of the nanocomposite films was evaluated using BET (NOVA Touch, Quantachrome, UK) by drying the samples at 100 ^{o}C for 12h using liquid nitrogen for the measurements. In addition, thermal characterisation of the nanocomposites was performed to study the interface between the PVC-grafted nanoparticles and the polymeric films. Differential Scanning calorimetry (DSC) (N5370212, Perkin Elmer, US) was conducted to establish the glass transition temperature of the nanocomposite sensing films. Such analysis was conducted between 40 and 200 ^{o}C at a rate of 10 ^{o}C/min. Thermogravimetric analysis (TGA) (N5370210, Perkin Elmer, US) was employed to confirm the grafting of the carboxylated PVC onto the functionalised silica nanoparticles. In this case, the nanocomposite sensing films were subjected to a temperature between 30 – 650 ^{o}C at a rate of 10 ^{o}C/min and the weight change was monitored. Nanoindentation (NanoTest Vantage, Micromaterials, UK) was employed to test the hardness of the nanocomposites with different degrees of cross-linker. A maximum force of 100 mN was applied onto the surface of the films using a Berkovich tip and a hardness map was then generated by performing a matrix of indentations with each point being separated by 2 μm. The results were represented in the form of a microhardness map, showing local aggregation of nanoparticles.

2.6 Study of the ionic exchange of the nanocomposite sensing film.

The ionic absorption was quantitatively determined using a quartz microbalance (Q-sense, Biolin Scientific, Sweden). This technique allows the quantification of the total mass change associated

with the ion diffusion from the water sample inside the nanocomposite sensing films. In this case, 10 µm thick nanocomposite sensing films were deposited onto gold electrodes by AACD under the abovementioned conditions. The films weight was then monitored after immersion in water and KCl for 2h. To determine the relative ion intake, the differences in the weight after equilibration in water for 2h and immersion in 0.1 M KCl for 2 h were calculated and divided by the original weight (equation 1).

$$RI = \frac{(W_{Ion} - W_{film})}{W_{film}} \quad (1),$$

Where RI is the relative ion intake, W_{Ion} the weight after equilibration in 0.1 M KCl for 2h and W_{film} the weight after equilibration in water for 2h. The measurement was repeated for the immersion of the film in $CaCl_2$. for 2h

2.7 Electrochemical characterisation of the devices

The measurement of the potentiometric response was conducted by using an AUTOLAB. In all cases, the open circuit potential (OCP) was recorded after subjecting the sensors to different concentrations of KCl and $CaCl_2$ independently in the range of 10^{-9} up to 10^{-1} M. Firstly, films containing PVC-grafted silica nanoparticles with the use of different amount of EDC/NHS crosslinkers during their synthesis with and without valinomycin ionophores were characterised. This study allowed the determination of the effects of the PVC-grafted silica nanoparticles on the ion intake of the PVC polymeric films alone. The sensitivity towards both electrolytes employed in this study was determined by measuring the slope of the calibration curves. In addition, the sensitivity after the use of ionophores was recorded to evaluate the performance of the full sensing device.

2.8 Continuous testing of the sensing devices in a fluidic chamber setup

To further test the implications of mechanical resilience of the nanocomposite sensing films due to the higher hardness, a custom-made fluidic chamber was fabricated using additive manufacturing so that pressure and shear stress could be continuously applied via continuous flow.

In this case, a model was generated using Sketchup for the 3D printing of a fluidic with a channel of 2 x 7 cm, and 300 μm height by a Ultimaker 2+ using polylactic acid. A peristaltic pump was used to provide a continuous water stream. After the sealing of the sensors deposited onto silica glass using PDMS, a flow rate of 60 mL min^{-1} was employed, corresponding to a pressure of 45 mbar, and the open circuit potential signal was recorded continuously using an AUTOLAB (PGSTAT128N, Metrohm, UK) for 8h.

To test the feasibility of the system for measuring the concentration of electrolytes in biological environments, the sensors were immersed in a solution containing simulated body fluids. Such solution is commercially available and contains a known concentration of ions. This solution was spiked with 500 μM KCl and the OCP of the sensors was determined and used to calculate the concentration of potassium ions by extrapolation. Finally, the sensors were immersed in human serum and the concentration of electrolytes was then determined similar to the case of the simulated body fluids.

3. RESULTS AND DISCUSSION

3.1 Characterisation of the functionalised nanoparticles

Initially, the grafting of carboxylated PVC polymer onto amined functionased fused silica nanoparticles (circa 7nm) was characterised using FTIR and TGA to confirm the presence of the grafted polymers and study their surface properties. Nanoparticles were grafted with 100 mg of carboxylated PVC (containing 1.8 wt% of carboxylic groups) using different amounts of EDC/NHS crosslinkers during the synthesis. Different concentrations (e.g. 16, 32, 49, 65, and 81

mM) of both EDC/NHS were added for the reaction, and the samples were labelled as 0, 20, 40, 60, 80 and 100% grafting degree since such concentrations were calculated from the amount of carboxylic groups present on the molecular structure of the employed PVC (Figure 2.a)). In this case, 100% grafting degree indicated a ratio of 1:1 of carboxylic groups to EDC/NHS crosslinkers. The EDC/NHS reaction with carboxylated PVC allowed the formation of a covalent bond between the silica nanoparticles and the PVC polymers mediated by the APTES functional groups present on the surface of such silica nanoparticles. The success of such grafting was confirmed by FTIR, showing the characteristic peaks of PVC at 2900 cm^{-1} and 1500 cm^{-1} due to the presence of -CH_2 groups in the PVC structure. In the case of functionalised nanoparticles, the amide stretches in due to the EDC/NHS cross-linking were present in the range of 1650 cm^{-1} [42]. Such peak position was a consequence of the influence of the carbonyl group (-C=O) also observed in multiple biopolymers [43, 44]. In addition, the stretches at 470 and 1100 cm^{-1} due to the siloxane Si-O-Si bridges were observed in the polymer-grafted silica samples [45, 46] (Figure 2.b)). In addition, the use of TGA allowed the confirmation of the presence of PVC polymeric chains on the silica nanoparticles by allowing a calculation of its relative mass after heating. Here, mass losses were obtained at 650 ^{o}C that were attributed to degradation of the PVC on the surface of the nanoparticles due to the high thermal stability of the silica as compared to this polymer at such temperature (Figure 1.c). A 6.8% weight loss was observed when silica nanoparticles that only contained an amine APTES functionalisation with no PVC polymers were studied, which is indicative of the presence of these aminated APTES groups and no anchoring of PVC chains. On the contrary, an 83.4% of weight loss was measured for 100% polymer-grafted nanoparticles after testing in the same conditions, indicating a high presence of PVC chains on the surface of these nanoparticles. A non-complete grafting reaction was found in the 20% polymer-grafted nanoparticles, which only showed a weight loss of 43%, due to the lower amount of cross-linker being employed.

The hydrophobicity of the polymer-grafted silica nanoparticles changed as a consequence of the functionalisation. Here, the theoretical hydrophobicity of the surface of the PVC polymer-grafted silica nanoparticles was calculated by applying the same functionalisation process onto a flat silica surface as a reference material. Similar models with flat silica for the study of the surface properties of the nanomaterials have been previously used for the optimisation of surface reactions of silanization using APTES [47]. The water contact angle of the silica surface after functionalisation was found to increase as the degree of polymer functionalisation was higher (Figure 2.d)), from 43.3±1.4^{o} in the case of the 0% PVC grafted silica, containing aminated APTES, up to 79.6±1.6 ^{o} when glass with 100% degree of PVC grafting.

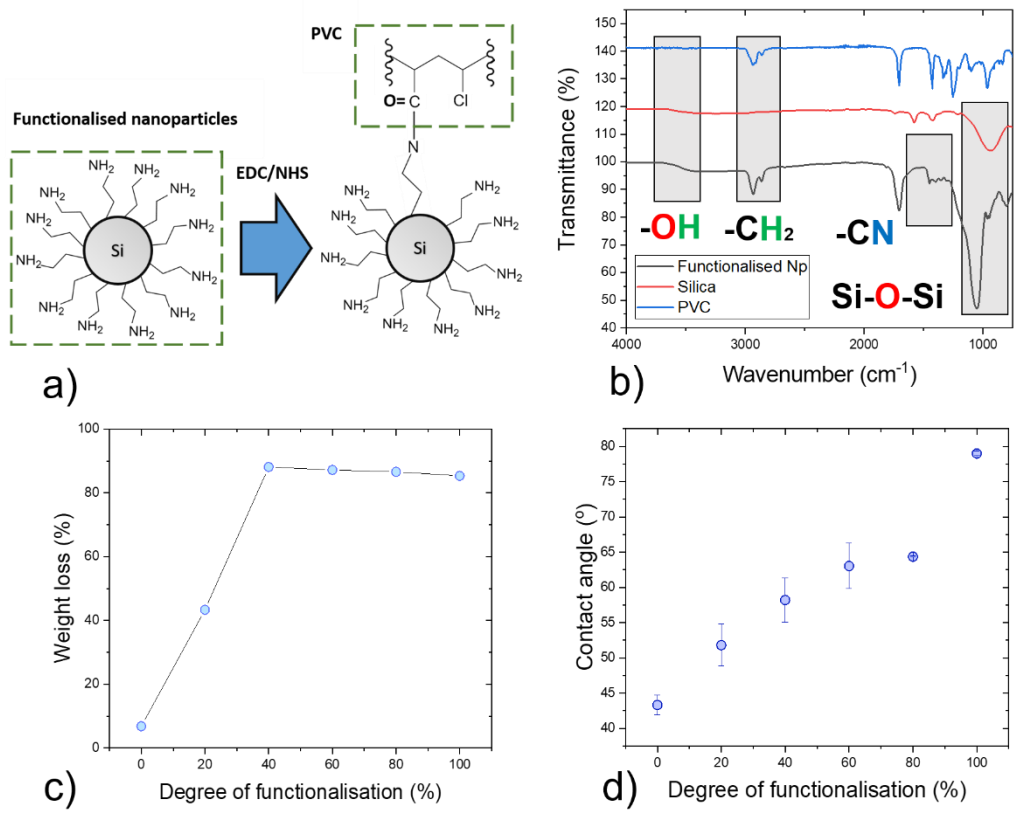

Figure 2. a) Schematic representation of the carboxylated PVC grafting onto APTES functionalised silica nanoparticle, where carboxylated PVC was used as a capping agent. The degree of grafting varied depending on the concentration of EDC/NHS, from 0 to 81 mM. **b)** The FTIR spectrum for 100% PVC grafted on silica nanoparticles as compared with the one obtained from its pure components, confirming the grafting of PVC by the presence of 100% degree of functionalisation. **c)** Mass variation of the polymer-grafted silica after subjecting them to 650 ºC, where the mass increases as the degree of grafting was higher. A maximum grafting was obtained at 40% of grafting of carboxylated PVC onto aminated silica nanoparticles, while the weight loss was similar from 60 – 100%. **d)** Contact angle measurement of flat silica glass surface after grafted with carboxylated PVC using different quantities of EDC/NHS linkers.

3.2 Study of the effects of silica nanoparticles on the nanocomposite films

The surface morphology of the nanocomposite films was characterised to establish the suitability of the AACD deposition process for the development of nanocomposite sensors with well

controlled structure, composition and thickness. The deposited nanocomposite sensing films were uniform and exhibited a high surface homogeneity as shown in the AFM image, with a low surface roughness, in the range of 9.6 nm (Figure 3.a)). In all cases, films with a typical thickness of circa. 5 µm were deposited. This high degree of homogeneity was essential for the systematic study of the electrochemical and mechanical properties of different nanocomposite films here, as this would allow a reduction of the errors derived from the interfacial resistance of the electrodes [48], which can limit the sensitivity of the sensors.

For the evaluation of the physical-chemical effects of PVC grafting on silica nanoparticles in the polymeric electrodes, two fundamental properties of the materials were studied: the glass transition temperature; and hardness of the films. The glass transition temperatures of polymers and nanocomposites affect the mechanical properties and the interaction of nanoparticles with the polymers. In general, a high glass transition temperature leads to elevated hardness values [49]. Such increase in the hardness is a consequence of the interaction strength between the nanoparticles and the polymers [50, 51], with a high glass transition temperature being indicative of a high interfacial energy [50]. Thus, the limitations in the mechanical hardness of the films due to the use of plasticizer PVC were circumnavigated by the integration of polymer-grafted nanoparticles that increased the glass transition temperature of the blends (Figure 3.b)). Consequently, the hardness of the sensing films and the Young modulus increased with the degree of grafting (Figure 3.c) and Figure 3.d)).

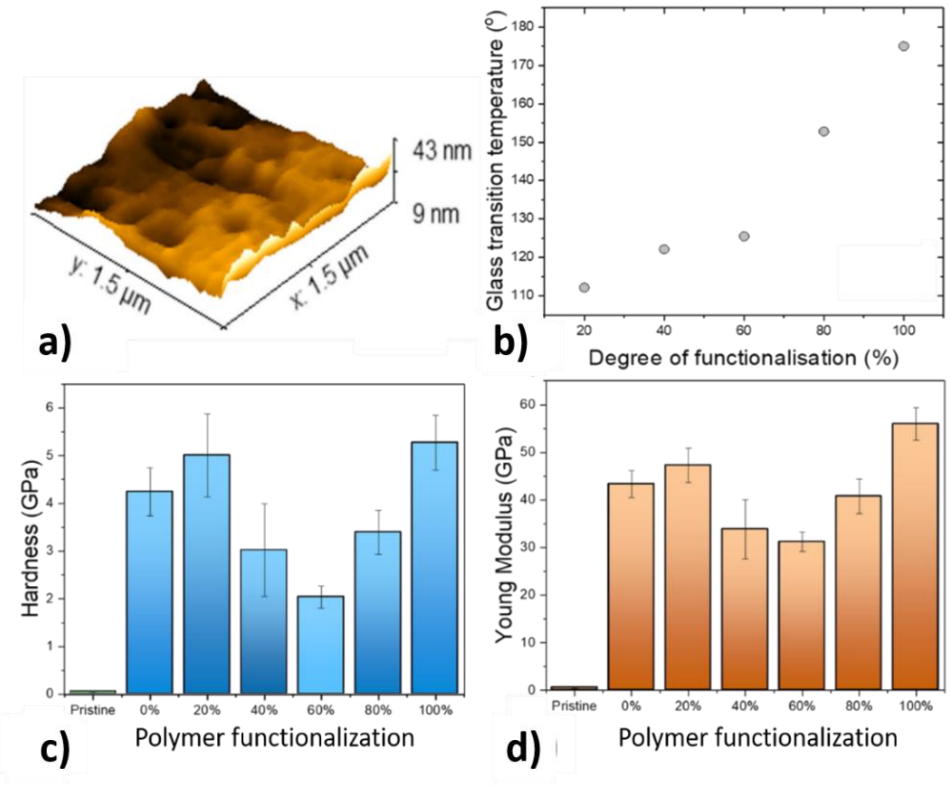

Figure 3. a) AFM image of the nanocomposite sensing films containing 100% PVC grafted onto silica nanoparticles and deposited by AACD. **b)** DSC plot of the nanocomposites with different degree of PVC grafting. **c)** Mechanical hardness of polymeric nanocomposites using variable degree of PVC functionalisation. In all cases, a higher hardness value was obtained as compared to the control pristine sample, where no silica nanoparticles were incorporated into the plasticized PVC. Due to the local aggregations, a high heterogeneity on the surface hardness was obtained in the nanocomposite sensing films due to the formation of nanoparticle aggregates, which was reflected in the obtained errors. **d)** Young Modulus of the nanocomposite sensing films measured by micro indentation.

The hardness and elasticity of the sensing films decreased within the 20-60% range, However, it increased at higher degrees of functionalisation, reaching 5.2±0.5 GPa when 100% polymer functionalisation was employed. The effect of nanoparticles on the glass transition temperature of the nanocomposite was attributed to the local interaction between the grafted PVC polymer

anchored onto the functionalised silica nanoparticles and the PVC polymeric matrix, which became stronger as the degree of grafting increased. In fact, a similar observation of a higher transition temperature of nanocomposite containing more polymer-grafted nanoparticles has been demonstrated by Hu *et al.* [52] using polymide-grafted silica nanoparticles in a nanocomposite containing poly(amic acid) matrix. On the contrary, the differences observed in the hardness upon the use of different functionalisation were attributed to the presence of nanoparticle aggregates. This effect has been reported for multiple polymer/spherical nanoparticle systems, where the presence of aggregates resulted in deleterious effects on the hardness of the films [53]. In our case, a good dispersion of nanoparticles was obtained at 0 and 20%. However, at such functionalisation degrees, a non-complete attachment of PVC chains onto the nanoparticles was obtained, reducing the interaction strength between the nanoparticles and the polymeric matrix. When a complete functionalisation was achieved, the nanoparticles aggregated, decreasing the hardness of the films. Silica is a ceramic material with a high hardness as compared to PVC polymers. However, the interaction of silica with the PVC polymeric chains present in the sensing film is relatively weak compared to the strong dipole-dipole interactions of PVC (Figures 4.a) and 4.b)) [54]. Thus, the functionalisation with PVC could enhance such interaction and increase the hardness of the films. However, the formation of aggregates can weaken this interaction, leading to suboptimal mechanical properties of the films. The effect of the formation of such aggregates could be observed by performing successive indentations with a spacing of 2 µm, creating the microhardness map (Figure 4.c-i)).

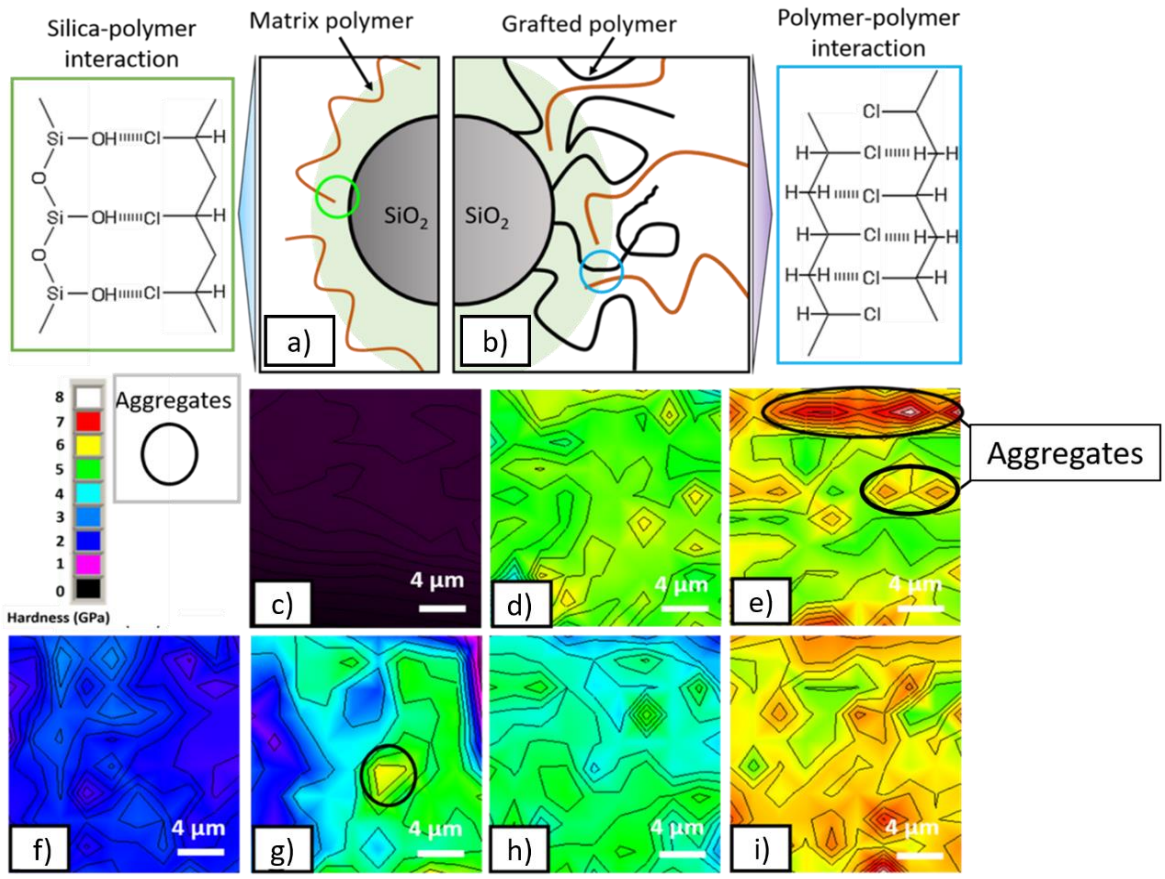

Figure 4. a) Schematic representation of the silica-PVC interaction on the surface of the nanoparticles. **b)** PVC-PVC interaction taking place at the surface of the functionalised nanoparticles grafted with carboxylated PVC. **c)** Hardness mapping of pristine plasticized PVC films. **d-i)** Micro hardness mapping of films incorporated with 5 w.t% of 0, 20, 40, 60, 80, and 100% polymer grafted silica nanoparticles. The presence of nanoparticulate aggregates is indicated.

The indentation map allowed a visualization of the hardness homogeneity across the surface of the films, which was influenced by the presence of nanoparticle aggregates. A homogeneous dispersion of polymer-grafted silica nanoparticles was observed at a high degree of grafting due to the better dispersion of these nanoparticles in the precursor solution. However, the presence of large aggregates was observed reduce the hardness of the films as reflected in the indentation maps. This result of the effects of functionalisation on the size of the aggregates was corroborated by

DLS (Figure 5.a)), where a maximum size of 837±83 nm was observed in the case of 60% functionalised nanoparticles, which was the film with the lowest hardness. Such dispersion was driven by the higher presence of PVC polymeric chains. This effect has previously observed in other polymer-grafted materials (e.g. carbon nanotubes), where the grafting of polymeric chains can improve their dispersion inside a polymeric matrix [39].

The presence of silica nanoparticles not only had an impact on the hardness of the films, but also it could be used to tune the microstructure of the sensing films. In order to determine how the sensing films were influenced by the microstructure y of the nanocomposites, SEM imaging was conducted on the cross-section of the plasticized PVC films (Figure 5.b)), and compared with the 100% PVC grafted silica nanoparticles reinforced PVC nanocomposite (Figure 5.c)).

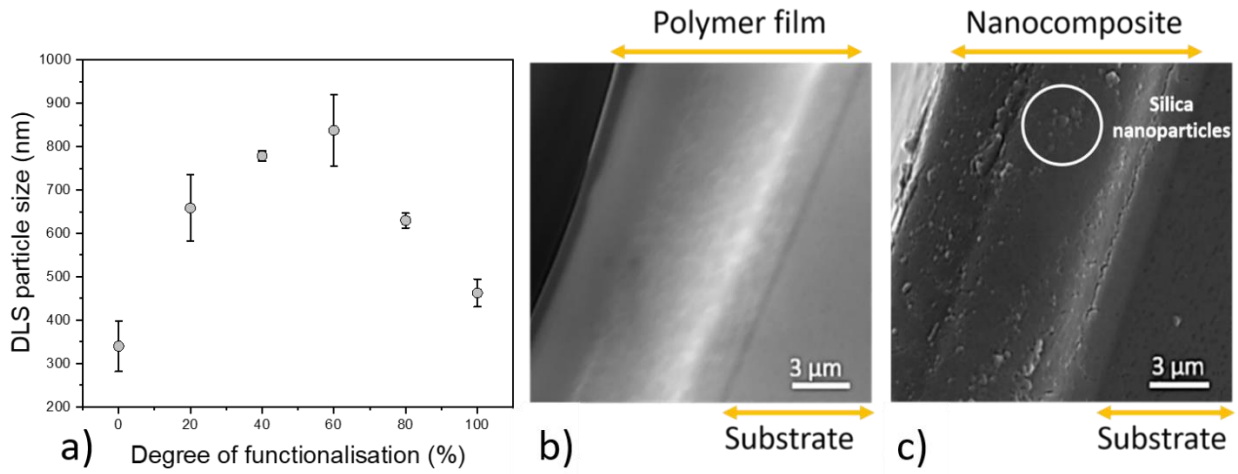

Figure 5. a) Mean particle size of the PVC-functionalised silica nanoparticles dispersed in cyclohexanone as the precursor solution calculated from DLS. A higher presence of particle aggregates was observed in the case of 60% functionalised silica nanoparticles. Results were taken by triplicates. **b)** Cross-sectional SEM image of the standard plasticized PVC polymeric film. **c)** Structure of the nanocomposite sensing film containing 100% PVC grafted onto silica nanoparticles.

In the case of the standard plasticized PVC polymeric film, a 10 µm thick dense polymer film was observed. This dense microstructure was a product of the combination of the PVC and the

plasticizer, that created a compact layer with low porosity and a pore radius in the range of 1.33±0.07 nm as measured by BET. In addition, the presence of small striations due to the presence of plasticizer was observed by SEM. On the contrary, a higher presence of interconnected channels was evidenced when the films contained 5 w.t% of 100% PVC grafted silica nanoparticles. Such increase in porosity was a consequence of the presence of the nanoparticles as confirmed by BET. In this case, the pore radius of the nanocomposite sensing varied from 1.66±0. 8 nm using 20% PVC grafted silica nanoparticles up to 4±2 nm when 100% PVC grafted silica nanoparticles were incorporated into PVC matrix. This increase in the porosity of the films improved the electrochemical performance of the ion-selective electrodes by facilitating the diffusion of potassium ions as observed in section 4.3.

3.3 Electrochemical characterisation of nanocomposites

The impact of the silica nanoparticles in the ionic diffusion of the nanocomposites and electrochemical interferences due to secondary electrolytes was determined by measuring the potentiometric response of the electrodes without the use of ionophores. Concentrations from 10^{-8} up to 10^{-1} M of both KCl and $CaCl_2$ were employed and the open circuit potential of the sensors was measured. A calibration plot was obtained and the sensitivity was determined by measuring the slope of this plot within the linear range (Figure 6.a).

In this case, the sensitivity of the films towards K^+ ions decreased from 18.7±0.2 mV Log[K^+] when 0% of PVC grafting up to 2.3±1.0 18.7±0.2 mV Log[K^+]$^{-1}$ at 100% of PVC grafting. On the contrary, the potentiometric response towards Ca^{2+} ions remained constant, from 15.2±4.1 mV Log[Ca^{2+}]$^{-1}$ at 0% polymer grafting up to 12.3±1.4 18.7±0.2 mV Log[Ca^{2+}]$^{-1}$ at 100% of polymer grafting. Such phenomenon could initially be caused by 2 factors: a limitation of the ionic transfer from the sample into the nanocomposite, which could decrease the amount of positively charged cations diffusion to the polymeric films, thus reducing the sensitivity of the sensors; or an improved

diffusivity of counterions. The co-diffusion of negatively charged chloride ions could also reduce the sensitivity by countering the charges of the cations [55].

To determine the true nature of the changes in sensitivity upon different degree of grating of silica nanoparticles, the ion intake of the nanocomposite films in terms of mass absorption of the sensors was quantitatively assessed by using a quartz microbalance (Figure 6.b). This test allowed the evaluation of the total mass variations within the polymer film which could vary due to the co-diffusion of the target ions with their counterions (Cl^-), which are charged ions that can reduce the sensitivity of the films since they balance the potential increase due to the retention of cations (Figure 6.b). A positive correlation between the degree of grafting and the intake of KCl as measured by quartz microbalance was observed. On the contrary, the diffusion of $CaCl_2$ was reduced with the grafting of polymer which was evidenced by a lower relative ion intake. Thus, the use of 100% grafting of polymer onto amine functionalised silica nanoparticles in the plasticized PVC films improved the permeability of K^+ along and with the Cl^- anions, increasing the total mass but reducing the potentiometric sensitivity since such chloride anions can counter the charge of the potassium cations. However, when valinomycin ionophores were integrated in the sensing films, a reproducible Nernst sensitivity response was obtained, with a limit of detection in the range in the range of 10^{-4} M. Such sensitivity was corroborated by fabricating 3 different electrode batches and calibrating the films against different concentrations of KCl (Figure 6.c). The effect of the porosity on the performance of ion-selective electrodes was a consequence of the improved porosity of the films and the higher hydrophobicity of the nanoparticles as compared to the pristine films (Figure 6.d and Figure e).

Hydrophobic nanochannels have been proven to favour the selectivity of ion sensors selective towards large ions such as K^+ due to their low hydration energy, in the range of -372 kJ mol^{-1} as compared with bivalent ions such as Ca^{2+}, with -1656 kJ mol^{-1} [56]. Consequently, the ion transfer of K^+ from the sample solution to the sensing film requires less energy than the transfer of Ca^{2+}

ions [57]. In this case, the bigger pore radius of the films, 7±2 nm when 100% PVC polymer grafted silica nanoparticles were incorporated into the PVC matrix, also increased the diffusion of Cl^- ions. As a consequence, the sensitivity of the electrodes towards calcium ions was reduced. However, such effect did not alter the sensitivity of the devices towards KCl after the use of ionophores. This was demonstrated by comparing the performance of a conventional device containing a plasticized PVC film with valinomycin as the ionophore, and a different device with 100% polymer grafted silica nanoparticles and valinomycin ionophore. In both cases, the sensors showed a standard Nernstian response (Figure 6.f). To determine the stability of the measurements and the response of the sensing devices under different concentrations of electrolytes, the sensors were subjected to a hysteresis test. In this case, the devices were first stabilised in a solution containing 10 mM KCl for at least 10 mins. The devices were then immersed in a solution containing 1 mM $CaCl_2$. As a consequence of the no presence of KCl in such solution, the OCP of the sensors decreased. After re-immersing the sensors in the solution containing 10 mM KCl, a OCP signal similar to the one obtaining during the stabilisation was obtained, indicating a good performance of the sensing devices (Figure 6.g).

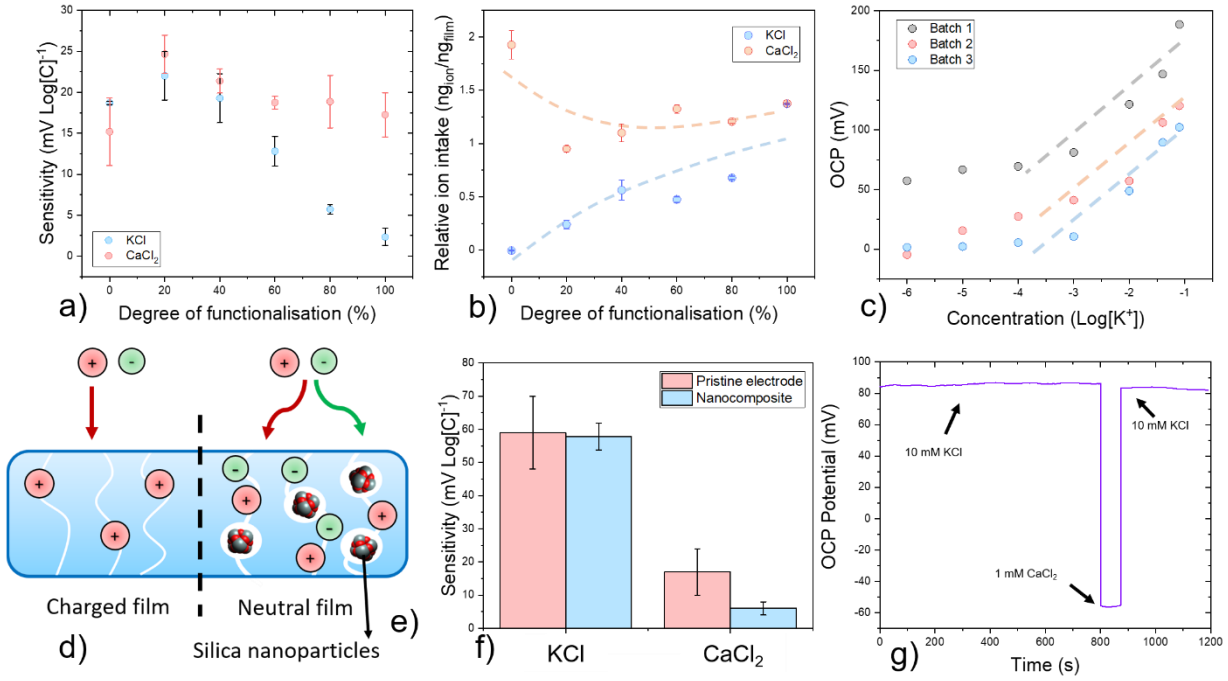

Figure 6. a) Potentiometric sensitivity of ion-selective electrodes where 5 wt% of functionalised nanoparticles were incorporated into a plasticized PVC film. **b)** Relative mass absorption of the nanocomposite sensing film containing the PVC-grafted silica nanoparticles, measured by a quartz microbalance after exposure to potassium and calcium ions. **c)** Reproducibility testing of the ion sensors by measuring the sensitivity of 3 devices fabricated in 3 different batches. **d)** Ion diffusion model inside the polymeric films with no nanoparticle incorporation. When no nanoparticles are present, only the diffusion of cations is favoured. Only one of the ionic species can diffuse from the aqueous sample to the polymer film in this case. **e)** When polymer-grafted silica nanoparticles are incorporated into the PVC film, the diffusion of smaller counterions from the aqueous sample to the polymer film is favoured due to the larger pore size within the nanocomposite. **f)** Sensitivity of the sensors towards potassium and calcium ions of the conventional pristine (i.e. standard electrode) and nanocomposite sensing films. **g)** hysteresis effect study of the ion-selective electrodes incorporating 100% PVC functionalised nanoparticles.

After the calibration of the final devices using valinomycin as K^+-selective ionophore inside the plasticized PVC film, a sensitivity of 59±11 mV Log$[K^+]^{-1}$ was observed in the case of sensing

films with no nanoparticles. This value was aligned with the Nernst-sensitivity, which is the standard of performance of ion-selective electrodes, and has been reported by multiple studies in the field [14, 58]. This value was comparable to the one found in the films with 100% polymer-grafted silica nanoparticles inside the ion sensors, where 58±4 mV Log[K^+]$^{-1}$ was obtained, as measured by triplicates using 3 different batches of sensors. However, an improved selectivity towards K^+ as compared to Ca^{2+} was obtained in the case of 100% polymer-grafted silica nanoparticles inside the ion sensors. These sensors showed a sensitivity of 6±2 mV Log[Ca^{2+}]$^{-1}$ towards Ca^{2+} ions while the pristine version with no nanoparticles incorporated presented a sensitivity of 17±7 mV Log[Ca^{2+}]$^{-1}$.

The high porosity and hydrophobicity of the sensing nanocomposite films due to the presence of 100% polymer-grafted nanoparticles was then showed to be a promising element to reduce the interferences, decreasing the sensitivity towards calcium ion, by almost 3 times respect to the traditional approach while maintaining a comparable sensitivity towards potassium ions. The lower errors in the case of sensing nanocomposite films also indicated a lower electrochemical; noise compared to the conventional polymer-based approach.

The selectivity coefficients of the sensing devices were additionally determined by the fixed interference method as reported elsewhere [59]. In this case, 0.1 M of the interference electrolyte was employed, and the concentration of KCl was increased (Figure S.1). This test could be used to calculate the selectivity towards Na^+ ($k^{pot}_{K^+,Na^+} = -2.35$) and Ca^{2+} ($k^{pot}_{K^+,Ca^{2+}} = -3.6$). The selectivity of the devices towards potassium when compared to sodium was comparable to the results obtained by Sanggil *et al.* [60], employing similar film compositions without the addition of polymeric nanoparticles. Such selectivity was in the range of $k^{pot}_{K^+,Na^+} = -2.5$. In the case of calcium ions, the selectivity was higher than the reported values in the literature for valinomycin

ionophores ($k^{pot}_{K^+,Ca^{2+}} = -2.6$) [61, 62]. Thus, the benefits of the implementation of PVC-functionalised silica nanoparticles could were demonstrated.

4.4 Performance evaluation of sensing nanocomposites under dynamic testing conditions using a 3D printed fluidic chamber configuration

To date, typical ion-selective electrodes based on pristine plasticized PVC are tested under static conditions, with no movement of the aqueous electrolyte solution, being unrepresentative of their use in real-world situations such as marine environments or wearable technologies, where there is an effect of friction due to the continuous fluid flow or contact of the sensors with the skin.

The present approach using polymer-grafted nanoparticles can tackle this challenge, by improving the mechanical resilience of the films through a higher hardness. To further demonstrate the performance superiority of the nanoparticle incorporation in terms of electrochemical performance and mechanical resilience, a custom-made fluidic device was designed to test the performance of the sensors (Figure 7.a). This device was developed by using additive manufacturing techniques and applied a pressure of 45 mbars in the fluidic channels. Such pressure is similar to the one commonly found in human capillaries, which is in the range of 46.6 mbar [63]. As such, it represented a good model for the testing of the ion sensors in these environments.

Microfluidics represent a promising alternative for the development of fast high-performance sensors due to the improve diffusivity of analytes [64]. Consequently, they have been employed in multiple sensing modalities for the determination of biomarkers and electrolytes in solution [65, 66]. However, their use in combination with ion-selective electrodes sensors have been hindered by the mechanical constraints, due to the low hardness of the plasticized PVC films, and the high thicknesses achieved by the traditional drop casting technique, typically in the range of 100 µm [67]. Whereas the present work the use of polymer-grafted silica nanoparticles can improve the

hardness to address this limitation. Here, a fluidic chamber was used as an objective test for the study of the degradation of the electrodes over time during high pressure and shear stress. The nanocomposite sensing films were shown to increase the lifespan of these sensors for at least 8 h under a continuous 60 mL min^{-1} flow conditions of 0.1M of KCl by improving the physical stability of the nanocomposite sensing films. The electrochemical performance of the pristine sensing films was then compared to the nanocomposite sensing films using 100% polymer grafted nanoparticles (Figure 7.b).

One of the potential application of the robust sensing device reported within the present work is related with the diagnosis of diseases. Given the high relevance of potassium ions in biological processes, small fluctuations on its concentration in serum could be indicative of cardiovascular diseases [68] or bad outcomes during chronic kidney disease [69]. To test the feasibility of the developed sensor for the evaluation of potassium concentrations in biological solutions, the devices were immersed in a commercially available simulated body fluid (SBF) solution (Figure 7.c)). The composition of such SBF is detailed in Table S1, and contained 5 mM of K^+. When the concentration of K^+ was estimated by extrapolation of the sensor signal with the obtained response, a concentration of 5.3±1.4 mM was obtained, being consistent with the concentration reported by the commercial suppliers. Upon spiking this solution with 500 µM of KCl, such concentration increased up to 5.7±1.4 mM. Thus, these results demonstrate the possibility of integrating the potassium-selective electrodes for the determination of potassium in biological solutions. A proof-of-concept of the implementation of this sensing device as implantable sensors was then conducted by measuring the concentration of potassium in human serum. The standard concentration of potassium ions in serum is comprised between 3.3-5.5. mM [70]. As a consequence of the narrow concentration range of this ion, highly accurate devices need to be designed. When using the ion sensors incorporating PVC-functionalised nanoparticles, a concentration of 6.6±1.3 mM was measured (Figure 7.d)). Such concentration was in the range of the normal levels in human serum.

Similar to the previous case with the SBF solution, the samples were spiked using 500 µM of KCl, and a concentration of 7.0±1.2 mM was obtained, being consistent with the added concentrations. As such, these results indicated a good performance of the developed sensors inside biological environments.

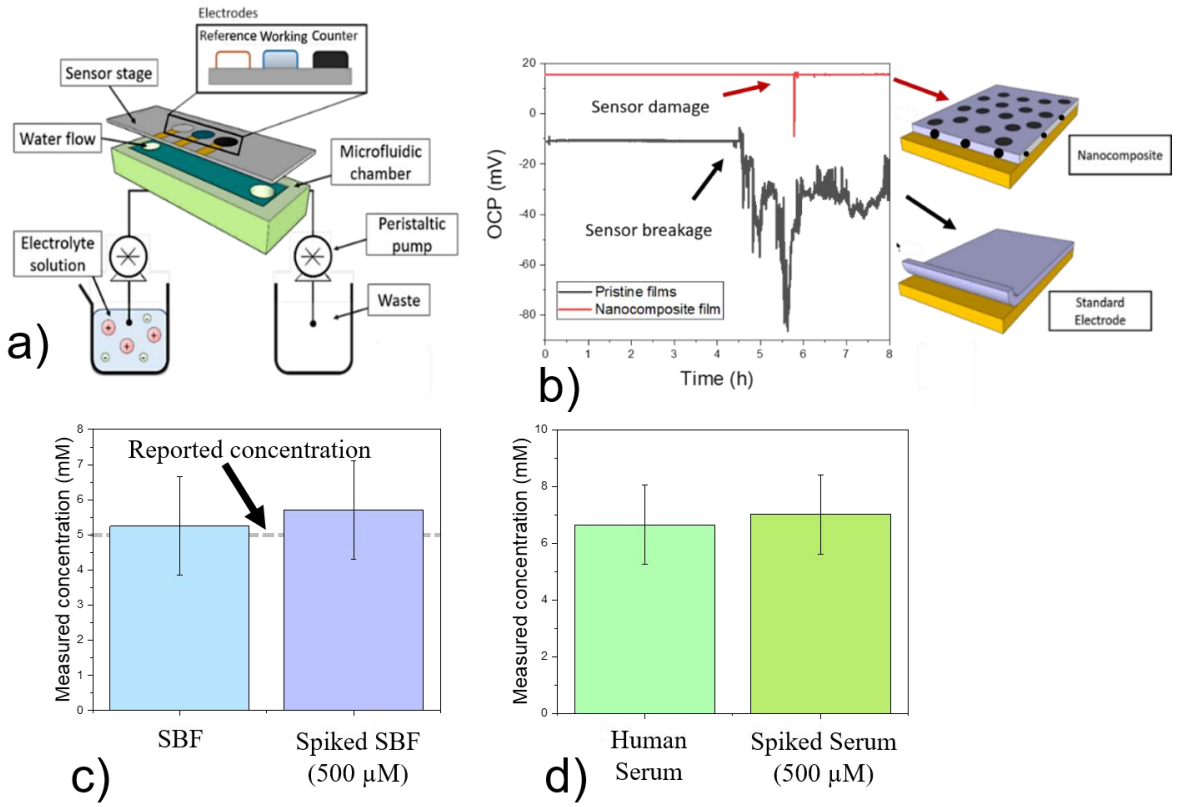

Figure 7. **a)** Schematic representation of the fluidic chamber employed. A 2 x 7 cm cavity with 300 µm thickness was fabricated by additive manufacturing, where the electrodes were placed and sealed using PDMS resin. An electrolyte solution was then pumped using a peristaltic pump at a flow rate of 60 mL/min. **b).** Potentiometric response of nanocomposites (red) and pristine (black) polymeric films subjected to a continuous flow of 60 mL min^{-1} containing 0.1 M of KCl for 8 h. The signal noise increased upon the film damage (as indicated with arrows). **c)** Concentrations measured in a SBF solution by the potassium-selective electrode with incorporated PVC-functionalised silica nanoparticles before and after spiking using 500 µM. The reported concentration by the manufacturers is also indicated. **d)** Concentrations measured in human serum by the potassium-selective electrode before and after spiking using 500 µM.

Regarding the stability of the sensing devices, in both cases, the potentiometric response remained constant within the initial time period. In the case of pristine films, the signal within the first hour presented a background noise of 115.6 μV h^{-1} while in the case of the sensor based on nanocomposite film it was 1.2 μV h^{-1}, one of the lowest values reported in the literature. This value is in the range of the stability as reported by Jinbo *et al.* [71], who holds the record of higher stability achieved in an ion-selective electrode of 1.3 ± 0.3 μV h^{-1} for up to 72 h. This value greatly increased in the pristine films after 4 h under 45 mbar of pressure, achieving 5.7 mV within the last tested hour. This is indicative of a damage in the film, resulting in an increase on the background noise due to the effect of water in the electrodes. Although some peaks can be observed in the case of nanocomposites sensing films after 5 h followed by a higher noise level, which is also indicative of a small degradation of the films due to the desorption of polymers from the film. However, the average drift after 8h of testing was 22.6 μV h^{-1}, significantly lower than the pristine ion-selective electrodes. These results indicated the higher time-stability and drift of these sensors compared to the pristine ion-selective electrodes, which is the standard approach in commercial devices.

5. CONCLUSIONS

Within the present work, the influence of the incorporation of polymer (e.g. PVC) grafted onto silica nanoparticles into the ubiquitously employed PVC-based ion-selective electrodes have been evaluated systematically, especially their impacts on the electrochemical and mechanical properties of the nanocomposite films. A novel and non-vacuum fabrication method, AACD, was employed for the development of highly homogeneous and smooth pristine PVC and nanocomposite films. A preferential intake of K^+ ions followed by a better specificity of the sensors towards this electrolyte as compared to Ca^{2+} was observed in the case of films with silica nanoparticles containing 100% polymer grafting as compared to the pristine films. The higher performance of these sensors was attributed to a higher porosity, where the mean pore radius

increased from 1.38±0.07 nm in the case of pristine sensing films up to 7±2 nm for 100% polymer grafted nanoparticles, and better selectivity of the films towards K^+. In addition, the use of polymer-grafted silica nanoparticles improved the harness of the films that allowed their integration within a fluidic configuration for the testing under dynamic conditions. This approach allowed the development of a highly robust in PVC nanocomposite sensing device with PVC-functionalised silica nanoparticles incorporated. Such device showed one of the lowest noise levels reported in the literature that could be integrated within a fluidic configuration for the monitoring of electrolytes for more than 8h under 45 mbar pressure. In addition, this sensor could accurately determine the concentration of K^+ inside complex mixtures of electrolytes, making it suitable for real-world applications. Such sensors were subjected to simulated body fluids, which presented a well-known concentration of electrolytes, and human serum, being able to accurately determine the concentration of K^+ in both cases, being in the range of 5 mM. This discovery will pave the way for the design of miniaturised wearable devices that can be used for the continuous monitoring of electrolytes with a minimum signal drift by tailoring the pore size and characteristics through different functionalised nanoparticles.

5. REFERENCES

1. Siswoyo, S., Zulfikar, and Asnawati, *Ion Selective Electrodes As Analytical Tools For Rapid Analysis of Soil Nutrients*. 2012.
2. Dhatt, G., Z. Talor, and A. Kazory, *Direct ion-selective electrode method is useful in diagnosis of pseudohyponatremia.* J Emerg Med, 2012. **43**(2): p. 348-9.
3. Sengupta, P., *Potential health impacts of hard water.* International journal of preventive medicine, 2013. **4**(8): p. 866-875.
4. Furness, J.B., *Types of neurons in the enteric nervous system.* Journal of the Autonomic Nervous System, 2000. **81**(1): p. 87-96.
5. Paparella, M.M., et al., *Cellular Events Involved in Middle Ear Fluid Production.* Annals of Otology, Rhinology & Laryngology, 1970. **79**(4): p. 766-779.
6. Dmitrieva, N.I. and M.B. Burg, *Elevated sodium and dehydration stimulate inflammatory signaling in endothelial cells and promote atherosclerosis.* PloS one, 2015. **10**(6): p. e0128870-e0128870.
7. Morrison, A.C. and R.B. Ness, *Sodium intake and cardiovascular disease.* Annu Rev Public Health, 2011. **32**: p. 71-90.

8. Hooper, L., et al., *Which Frail Older People Are Dehydrated? The UK DRIE Study.* The journals of gerontology. Series A, Biological sciences and medical sciences, 2016. **71**(10): p. 1341-1347.
9. Dahl, L.K., G. Leitl, and M. Heine, *Influence of dietary potassium and sodium/potassium molar ratios on the development of salt hypertension.* J Exp Med, 1972. **136**(2): p. 318-30.
10. Raebel, M.A., *Hyperkalemia Associated with Use of Angiotensin-Converting Enzyme Inhibitors and Angiotensin Receptor Blockers.* Cardiovascular Therapeutics, 2012. **30**(3): p. e156-e166.
11. Xiang, X., F. Pan, and Y.J.E.S. Li, *Flower-like Bismuth Metal-Organic Frameworks Grown on Carbon Paper as a Free-Standing Electrode for Efficient Electrochemical Sensing of Cd2+ and Pb2+ in Water.* 2018. **3**: p. 77-83.
12. Dong, Q., et al., *Heterogeneous Iridium Oxide/Gold Nanocluster for Non-enzymatic Glucose Sensing and pH Probing.* 2019. **8**: p. 46-53.
13. Kutyła-Olesiuk, A., et al., *Electrochemical Sensor Arrays for the Analysis of Wine Production.* Procedia Engineering, 2014. **87**: p. 580-583.
14. Gao, W., et al., *Fully integrated wearable sensor arrays for multiplexed in situ perspiration analysis.* Nature, 2016. **529**(7587): p. 509-514.
15. Valdastri, P., et al., *Wireless Implantable Electronic Platform for Chronic Fluorescent-Based Biosensors.* IEEE transactions on bio-medical engineering, 2011. **58**: p. 1846-54.
16. Yin, J. and S. Luan, *Opportunities and challenges for the development of polymer-based biomaterials and medical devices.* Regen Biomater, 2016. **3**(2): p. 129-35.
17. Geddes, W.C., *Mechanism of PVC Degradation.* Rubber Chemistry and Technology, 1967. **40**(1): p. 177-216.
18. Shahc, N., et al., *Fabrication of Thermally Stable Graphite-Based Poly(acrylonitrile-co-acrylic acid) Composite with Impressive Antimicrobial Properties.* 2019. **6**: p. 77-85.
19. Boni, B.O.O., et al., *Combining Silk Sericin and Surface Micropatterns in Bacterial Cellulose Dressings to Control Fibrosis and Enhance Wound Healing.* Engineered Science, 2020. **10**: p. 68-77.
20. Moody, G.J., B. Saad, and J.D.R. Thomas, *Glass transition temperatures of poly(vinyl chloride) and polyacrylate materials and calcium ion-selective electrode properties.* Analyst, 1987. **112**(8): p. 1143-1147.
21. Cuartero, M., G.A. Crespo, and E. Bakker, *Polyurethane Ionophore-Based Thin Layer Membranes for Voltammetric Ion Activity Sensing.* Analytical Chemistry, 2016. **88**(11): p. 5649-5654.
22. Malinowska, E., et al., *Enhanced electrochemical performance of solid-state ion sensors based on silicone rubber membranes.* Sensors and Actuators B: Chemical, 1996. **33**(1): p. 161-167.
23. Zahran, E.M., et al., *Polymeric plasticizer extends the lifetime of PVC-membrane ion-selective electrodes.* Analyst, 2014. **139**(4): p. 757-763.
24. Zareh, M., *Plasticizers and Their Role in Membrane Selective Electrodes*. 2012.
25. Xu, K., Y. Lu, and K. Takei, *Multifunctional Skin-Inspired Flexible Sensor Systems for Wearable Electronics.* Advanced Materials Technologies, 2019. **4**(3): p. 1800628.
26. Lu, D. and G.S. Kassab, *Role of shear stress and stretch in vascular mechanobiology.* Journal of the Royal Society, Interface, 2011. **8**(63): p. 1379-1385.
27. Moody, G.J., R.B. Oke, and J.D.R. Thomas, *A calcium-sensitive electrode based on a liquid ion exchanger in a poly(vinyl chloride) matrix.* Analyst, 1970. **95**(1136): p. 910-918.
28. Bloch, R., A. Shatkay, and H.A. Saroff, *Fabrication and evaluation of membranes as specific electrodes for calcium ions.* Biophysical journal, 1967. **7**(6): p. 865-877.
29. Das, R., et al., *Synthesis and Characterization of Antiflammable Vinyl Ester Resin Nanocomposites with Surface functionalized Nanotitania.* *ES Materials & Manufacturing*, 2020. **8**: p. 46-53.
30. Sun, L., et al., *Optimizing Strategy for the Dielectric Performance of Topological-structured Polymer Nanocomposites by Rationally Tailoring the Spatial Distribution of Nanofillers.* Engineered Science, 2020. **12**: p. 95-105.
31. Razavi Mehr, M., *An electrochemical Cr (III)-selective sensor-based on a newly synthesized ligand and optimization of electrode with a nano particle.* 2011.

32. Jaworska, E., et al., *Lowering the Resistivity of Polyacrylate Ion-Selective Membranes by Platinum Nanoparticles Addition.* Analytical Chemistry, 2011. **83**(1): p. 438-445.
33. Zhou, M., et al., *Effective Solid Contact for Ion-Selective Electrodes: Tetrakis(4-chlorophenyl)borate (TB–) Anions Doped Nanocluster Films.* Analytical Chemistry, 2012. **84**(7): p. 3480-3483.
34. Liberman, A., et al., *Synthesis and surface functionalization of silica nanoparticles for nanomedicine.* Surface Science Reports, 2014. **69**(2): p. 132-158.
35. Hou, P., et al., *Novel Superhydrophobic Cement-based Materials Achieved by Construction of Hierarchical Surface Structure with FAS/SiO2 Hybrid Nanocomposites.* ES Materials & Manufacturing, 2018. **1**: p. 57-66.
36. Alabi, A., et al., *Review of nanomaterials-assisted ion exchange membranes for electromembrane desalination.* npj Clean Water, 2018. **1**(1): p. 10.
37. Tong, X., et al., *Mechanism Exploration of Ion Transport in Nanocomposite Cation Exchange Membranes.* ACS Applied Materials & Interfaces, 2017. **9**(15): p. 13491-13499.
38. Girija, A.R., *12 - Medical Applications of Polymer/Functionalized Nanoparticle Systems*, in *Polymer Composites with Functionalized Nanoparticles*, K. Pielichowski and T.M. Majka, Editors. 2019, Elsevier. p. 381-404.
39. Lee, W.J., et al., *Interfacially-grafted single-walled carbon nanotube / poly (vinyl alcohol) composite fibers.* Carbon, 2019. **146**: p. 162-171.
40. Hu, J., et al., *Solid polymer electrolyte based on ionic bond or covalent bond functionalized silica nanoparticles.* RSC Advances, 2017. **7**(87): p. 54986-54994.
41. Choy, K.L., *Chemical vapour deposition of coatings.* Progress in Materials Science, 2003. **48**(2): p. 57-170.
42. F.S., P., *Amides and amines*, in *Applications of Infrared Spectroscopy in Biochemistry, Biology, and Medicine*. 1958, Springer, Boston, MA.
43. Ramesh, S., et al., *FTIR studies of PVC/PMMA blend based polymer electrolytes.* Spectrochimica Acta Part A: Molecular and Biomolecular Spectroscopy, 2007. **66**(4): p. 1237-1242.
44. Gu, H., et al., *Smart strain sensing organic–inorganic hybrid hydrogels with nano barium ferrite as the cross-linker.* Journal of Materials Chemistry C, 2019. **7**(8): p. 2353-2360.
45. Beltrán, M., J.C. García, and A. Marcilla, *Infrared spectral changes in PVC and plasticized PVC during gelation and fusion.* European Polymer Journal, 1997. **33**(4): p. 453-462.
46. Al-Oweini, R. and H. El-Rassy, *Synthesis and characterization by FTIR spectroscopy of silica aerogels prepared using several Si(OR)4 and R''Si(OR')3 precursors.* Journal of Molecular Structure, 2009. **919**(1): p. 140-145.
47. Howarter, J.A. and J.P. Youngblood, *Optimization of Silica Silanization by 3-Aminopropyltriethoxysilane.* Langmuir, 2006. **22**(26): p. 11142-11147.
48. Tran, T.N.T., S. Qiu, and H. Chung, *Potassium Ion Selective Electrode Using Polyaniline and Matrix-Supported Ion-Selective PVC Membrane.* IEEE Sensors Journal, 2018. **18**(22): p. 9081-9087.
49. Ebnesajjad, S., *Introduction to Plastics*, in *Chemical Resistance of Commodity Thermoplastics*, E. Baur, K. Ruhrberg, and W. Woishnis, Editors. 2016, William Andrew Publishing. p. xiii-xxv.
50. Chen, F., et al., *Glass Transition Temperature of Polymer–Nanoparticle Composites: Effect of Polymer–Particle Interfacial Energy.* Macromolecules, 2013. **46**(11): p. 4663-4669.
51. Khostavan, S., et al., *The Effect of Interaction between Nanofillers and Epoxy on Mechanical and Thermal Properties of Nanocomposites: Theoretical Prediction and Experimental Analysis.* Advances in Polymer Technology, 2019. **2019**: p. 8156718.
52. Hu, S.-N., Y. Lin, and G.-Z. Wu, *Nanoparticle Dispersion and Glass Transition Behavior of Polyimide-grafted Silica Nanocomposites.* Chinese Journal of Polymer Science, 2020. **38**(1): p. 100-108.
53. Zare, Y., *Study of nanoparticles aggregation/agglomeration in polymer particulate nanocomposites by mechanical properties.* Composites Part A: Applied Science and Manufacturing, 2016. **84**: p. 158-164.
54. Braun, D., B. Böhringer, and J. Herth, *Properties of poly(vinyl chloride) blends with polycarbonates and chlorinated polyethylene.* Makromolekulare Chemie. Macromolecular Symposia, 1989. **29**(1): p. 227-240.

55. Gemene, K.L., A. Shvarev, and E. Bakker, *Selectivity enhancement of anion-responsive electrodes by pulsed chronopotentiometry.* Analytica chimica acta, 2007. **583**(1): p. 190-196.
56. Marcus, Y., *Thermodynamics of solvation of ions. Part 5.—Gibbs free energy of hydration at 298.15 K.* Journal of the Chemical Society, Faraday Transactions, 1991. **87**(18): p. 2995-2999.
57. Moldenhauer, H., et al., *Effective pore size and radius of capture for K+ ions in K-channels.* Scientific Reports, 2016. **6**(1): p. 19893.
58. Hu, J., A. Stein, and P. Bühlmann, *Rational design of all-solid-state ion-selective electrodes and reference electrodes.* TrAC Trends in Analytical Chemistry, 2016. **76**: p. 102-114.
59. Mahmud, M.A.P., et al., *Recent progress in sensing nitrate, nitrite, phosphate, and ammonium in aquatic environment.* Chemosphere, 2020. **259**: p. 127492.
60. Han, S., et al., *Microfabricated Ion-Selective Transistors with Fast and Super-Nernstian Response.* 2020. **32**(48): p. 2004790.
61. Kim, H.J.H., J.W.; Birrell, S.J., *Evaluation of nitrate and potassium ion-selective membranes for soil macronutrient sensing* American Society of Agricultural and Biological Engineers, 2006. **49**(597-606).
62. Rechnitz, G.A., *Directions for ion-selective electrodes.* Analytical Chemistry, 1969. **41**(12): p. 109A-113a.
63. Feher, J., *5.10 - The Microcirculation and Solute Exchange*, in *Quantitative Human Physiology*, J. Feher, Editor. 2012, Academic Press: Boston. p. 508-518.
64. Tølbøl Sørensen, K. and A. Kristensen, *Label-Free Monitoring of Diffusion in Microfluidics.* Micromachines, 2017. **8**(11): p. 329.
65. Johnson, R.D., et al., *Microfluidic ion-sensing devices.* Analytica Chimica Acta, 2008. **613**(1): p. 20-30.
66. Luka, G., et al., *Microfluidics Integrated Biosensors: A Leading Technology towards Lab-on-a-Chip and Sensing Applications.* Sensors (Basel, Switzerland), 2015. **15**(12): p. 30011-30031.
67. Szigeti, Z., et al., *Approaches to Improving the Lower Detection Limit of Polymeric Membrane Ion-Selective Electrodes.* Electroanalysis, 2006. **18**(13-14): p. 1254-1265.
68. Kjeldsen, K., *Hypokalemia and sudden cardiac death.* Experimental and clinical cardiology, 2010. **15**(4): p. e96-e99.
69. Korgaonkar, S., et al., *Serum potassium and outcomes in CKD: insights from the RRI-CKD cohort study.* Clinical journal of the American Society of Nephrology : CJASN, 2010. **5**(5): p. 762-769.
70. Rastegar A. Serum Potassium. In: Walker HK, H.W., Hurst JW, *Clinical Methods: The History, Physical, and Laboratory Examinations. 3rd edition.* 1990.
71. Hu, J., et al., *Ion-Selective Electrodes with Colloid-Imprinted Mesoporous Carbon as Solid Contact.* Analytical Chemistry, 2014. **86**(14): p. 7111-7118.